On controlling the nonlinear vibrations of a Rectangular Thin Plate with Time delay feedback

Y. A. Amer*, A. T. EL-Sayed **, E. El Emam.Ahmed***

** Department of Mathematics, Faculty of Science, Zagazig University, Zagazig, Egypt*
*** Department of Basic Sciences, Modern Academy for Engineering and Technology, Egypt*
**** Department of Basic Sciences, Higher Technological Institute, 10th of Ramadan City, Egypt*
*Corresponding author. E-mail:basma00767@yahoo.com (*E. El Emam.Ahmed)

Abstract: In this paper, the time-delay feedback is applied to reduce the dynamic vibration of a rectangular thin-plate under external and parametric excitations. The equations of motion are determined by a von Karman type equation and Galerkin's method. The analytical solution is obtained by the technique of multiple time scales method (MTSM). The effect of control is studied to show the safe regions in which the system amplitudes can be decreased at some values of time delay. The system response is investigated numerically with and without time-delay feedback near-simultaneously internal and primary resonance $(\Omega_1 = \omega_1 = \omega_2)$ using the Runge-Kutta fourth-order (RK-4) method (package ode45 in Matlab R2014a). The stability of the nonlinear vibrating system is studied by using the frequency response equations according to the Routh-–Hurwitz criterion. The effects of different parameters on the system behavior are investigated numerically. Also, numerical simulations have a good agreement with the analytical solution. Finally, making a comparison with related previously published work.

Keywords: Rectangular thin-plate; Time-delay feedback; Multiple time scales method; Stability; Frequency-response function; Periodic solutions.

1. INTRODUCTION

In many engineering structures, rectangular thin-plates have been widely used, for example, large space stations and shuttles. These engineering applications received a lot of interest from scientists for studying and investigating undesirable vibrations that destroyed these thin-pates. (Zhang, 2001) studied the chaotic motion in thin-plates under parametric excitation and found chaotic motion in the full four-dimensional system. The multiple time scales method is used to get frequency response equations under simultaneously internal and primary resonance case. (Guo and Zhang, 2011) studied the attitude of chaotic motions in the nonlinear laminated rectangular thin-plate under parametric excitation forces. The nonlinear ordinary differential equation is solved by the Galerkin discretization approach. The perturbation solution is getting by the multiple timescales method near the 1:2:3 internal resonances. The Runge-Kutta of the fourth-order method is used to study the steady-state response at the chaotic dynamic of the laminated plate at the averaged equations. (Zhang et al., 2001) examined the thin-plate under external and parametric excitation at local and global bifurcations. The numerical simulation is used to get the chaotic motion of the thin-plate. (Kim, 2005) explained the nonlinear vibration of sheet metal plates with interacting parametric and external excitation during manufacturing. The system is represented by one degree-of-freedom with cubic non-linearity terms under combined parametric and external excitation forces. (Lai et al., 2009) interested in studying the asymptotic analysis for large-amplitude nonlinear free vibration of simply supported laminated plates. (Zhang and Li, 2010) used exponential dichotomies and an averaged procedure to the analyzed thin plate under external and parametric excitation at the resonant chaotic motions. (Sayed and Mousa, 2012) investigated the effect of non-linear dynamic characteristics of the angle-ply composite laminated rectangular plate having quadratic and cubic terms under combined excitations.

So, for many years the technique for reducing vibrations has been extensively studied in dynamic systems. Therefore, these vibrations may cau3se the risk of damage, disruption, and demolition for these dynamic systems. So, we can manage these vibrations by using various ways of vibration controls as active and passive control or time-delay feedback control. (Bauomy and El-Sayed, 2016) analyzed the chaotic motion of thin-plate by performing a comparison between four negative active controllers (Linear, Quadratic, Cubic, Acceleration) at the selected simultaneously primary resonance case $(\Omega_1 \cong \omega_1,\ \Omega_2 \cong \omega_2)$ and find the negative acceleration feedback controller is the better one to reduce the vibration dramatically without reaching to stability in the system performance.

The delayed feedback is one of the different essential methods for reducing vibrations in the dynamic system. (Zhao and Xu, 2007) studied the nonlinear dynamic system under external excitation and adding 0delayed feedback control to reduce the vibrations in 1:1 internal

resonance $(\omega_1 \cong \omega_2)$. (Amer et al., 2016) added delay feedback control to suppress the resulting vibrations of the Duffing oscillator under parametric excitation forces. At some values time delay is applied to reduce the vibration of the nonlinear system. (El-Ganaini and Elgohary, 2011; El-Gohary and El-Ganaini, 2012) applied the time delay control to manage the chaotic vibration of the dynamic system at the sub-harmonic and primary resonance case $(\Omega_j \cong 2\omega_1, \omega_2 \cong \omega_1, j = 1..3)$ under multi-parametric and external excitation forces. (El-Sayed and Bauomy, 2014) studied the system under multi-parametric excitation forces and added time-delay feedback to reduce the vibrations of helicopter blade flapping method and the effectiveness of controller is about $\mathrm{E}_a = 2.7 \times 10^5$ at simultaneous sub-harmonic and internal resonance case $(\Omega \cong 2\omega_1,\ \omega_2 \cong \omega_1)$. (El-Bassiouny, 2006; Liu and Lu, 2009) added time delay state feedback to the duffing oscillator system to reduce the vibration at the worst resonance case. (Gouskovet et al., 2002) used two interdependent delays for reducing the vibrations of a nonlinear dynamics machining system and found the effectiveness of the continuous cutting instability getting good results. (Wirkus and Rand, 2002) studied the dynamics of two coupled van der pol oscillators with time delay coupling for suppressing the oscillations in the dynamic system. The averaged method is used to slow-flow in three dimensions; also the stability analysis for the slow-flow is verified. (Saeed et al., 2013) applied time-delay controller to suppress the vibration of a nonlinear beam under parametric and external excitations. The method of multiple time scale is used to get the perturbation solution and the equations of frequency response at simultaneous internal and primary resonances case $(\Omega \cong \omega_1, \omega_1 \cong 2\omega_2)$.

In this paper, the time delay of a linear velocity feedback is added to decrease the dynamic vibration and improve the chaotic motion of a rectangular thin- plate under external and parametric excitations. The multiple scales method is applied to get the approximate solution up to first-order approximation. The stability analysis is obtained from the frequency response equations and investigated numerically near-simultaneously internal and primary resonance $(\Omega_1 = \omega_1 = \omega_2)$. Also, the outcomes of different parameters on the steady-state response of the system are studied and examined numerically.

2. FORMULATION OF THE BUCKLED THIN PLATE

From (Zhang, 2001; Zhang et al., 2001), we consider a simply supported four edges rectangular thin plate of length a, b and thickness h, respectively. The thin plate is subjected to transversal and in- plane excitations, simultaneously. We establish a Cartesian coordinate system as shown in Fig. 1a and the coordinate Oxy is established in the middle surface of the thin plate. It is supposed that u, v and w represent the displacements of a point in the middle plane of the thin plate in the x, y and z directions, respectively. The in-plane excitation of the thin plate can be expressed in the form $p = p_0 - p_1 \cos\Omega_2 t$. From the van Karman type (Chia, 1980), the equations of motion for the thin plate given as:

$$D\nabla^4 w + \rho h\frac{\partial^2 w}{\partial t^2} - \frac{\partial^2 w}{\partial x^2}\frac{\partial^2 \phi}{\partial y^2} - \frac{\partial^2 w}{\partial y^2}\frac{\partial^2 \phi}{\partial x^2} + 2\frac{\partial^2 w}{\partial x \partial y}\frac{\partial^2 \phi}{\partial x \partial y} + \mu\frac{\partial w}{\partial t} = F(x,y)\cos\Omega_1 t, \tag{1}$$

$$\nabla^4 \phi = Eh\left[\left(\frac{\partial^2 w}{\partial x \partial y}\right)^2 - \frac{\partial^2 w}{\partial x^2}\frac{\partial^2 w}{\partial y^2}\right], \tag{2}$$

where, ρ is the density of thin plate, $D = Eh^3/(12(1-v^2))$ is the bending rigidity, E is Young's modulus , v is the ratio of Poisson, ϕ is the stress function , the thickness of the plate is h and the coefficient of damping is μ . For a simply supported plate the boundary conditions are in the form:

$$\begin{aligned} w &= \frac{\partial^2 w}{\partial x^2} = 0 \quad at \quad \text{x=0, a,} \\ w &= \frac{\partial^2 w}{\partial y^2} = 0 \quad at \quad \text{y=0, b.} \end{aligned} \tag{3}$$

The boundary conditions achieved by the stress function ϕ may be presented in the following form:

$$u = \int_0^a \left[\frac{1}{E}\left(\frac{\partial^2 \phi}{\partial y^2} - v\frac{\partial^2 \phi}{\partial x^2}\right) - \frac{1}{2}\left(\frac{\partial w}{\partial x}\right)^2\right]dx = \delta_x$$
$$\text{and} \quad h = \int_0^b \frac{\partial^2 \phi}{\partial y^2}dy = p \quad at \quad x = 0, a. \tag{4}$$

$$v = \int_0^b \left[\frac{1}{E}\left(\frac{\partial^2 \phi}{\partial x^2} - v\frac{\partial^2 \phi}{\partial y^2}\right) - \frac{1}{2}\left(\frac{\partial w}{\partial y}\right)^2\right]dx = 0$$
$$\text{and} \quad \int_0^a \frac{\partial^2 \phi}{\partial x^2}dy = 0 \quad at \quad y = 0, b. \tag{5}$$

where δ_x is the corresponding displacement per unit length in the x direction at the boundary . The nonlinear oscillations of the rectangular thin plate are studied by the Galerkin method. So, we take into consideration the nonlinear oscillations of the rectangular thin- plate in the first two modes and the w is written in the form as follows

$$w(x,y,t) = u_1(t)\sin\left(\frac{3\pi x}{a}\right)\sin\left(\frac{\pi y}{b}\right) + u_2(t)\sin\left(\frac{\pi x}{a}\right)\sin\left(\frac{3\pi y}{b}\right), \tag{6}$$

where, $u_1(t),\ u_2(t)$ are the amplitudes of two modes. The transverse excitation can be written as

$$F(x,y)=F_1 sin\left(\frac{3\pi x}{a}\right)sin\left(\frac{\pi y}{b}\right)+F_2 sin\left(\frac{\pi x}{a}\right)sin\left(\frac{3\pi y}{b}\right), \tag{7}$$

where, F_1, F_2 specify the amplitudes of the transverse forcing excitation corresponding to the two nonlinear modes.

From equation (A6) into equation (A2), considering the boundary conditions (A4)–(A5) and integrating, we get the stress function in the following form:

$$\begin{aligned}\varphi(x,y,t)=&\phi_{20}(t)\cos\left(\frac{2\pi x}{a}\right)+\phi_{02}(t)\cos\left(\frac{2\pi y}{b}\right)\\&+\phi_{60}(t)\cos\left(\frac{6\pi x}{a}\right)+\phi_{06}(t)\cos\left(\frac{6\pi y}{b}\right)\\&+\phi_{22}(t)\cos\left(\frac{2\pi x}{a}\right)\cos\left(\frac{2\pi y}{b}\right)\\&+\phi_{24}(t)\cos\left(\frac{2\pi x}{a}\right)\cos\left(\frac{4\pi y}{b}\right)\\&+\phi_{42}(t)\cos\left(\frac{2\pi x}{a}\right)\cos\left(\frac{2\pi y}{b}\right)\\&+\phi_{44}(t)\cos\left(\frac{4\pi x}{a}\right)\cos\left(\frac{4\pi y}{b}\right),\\&-\frac{1}{2}py^2\end{aligned} \tag{8}$$

Where

$$\begin{aligned}&\phi_{20}=\frac{9Eh}{32\lambda^2}u_1^2,\phi_{02}=\frac{9\lambda^2Eh}{32}u_2^2,\phi_{60}=\frac{Eh}{288\lambda^2}u_2^2,\\&\phi_{06}=\frac{\lambda^2Eh}{288}u_1^2,\phi_{22}=-\frac{\lambda^2Eh}{(\lambda^2+1)}u_1u_2,\\&\phi_{24}=\frac{25\lambda^2Eh}{16(\lambda^2+4)^2}u_1u_2,\phi_{42}=\frac{25\lambda^2Eh}{16(4\lambda^2+1)^2}u_1u_2,\\&\phi_{44}=-\frac{\lambda^2Eh}{16(\lambda^2+1)}u_1u_2,\lambda=\frac{b}{a}.\end{aligned} \tag{9}$$

To get the dimensionless equations, the transformations of variables and parameters are presented as the following

$$\begin{aligned}&\bar{x}_i=\frac{(ab)^{1/2}}{h^2}u_i(i=1,2),\ \bar{F}_i=\frac{(ab)^{5/2}}{\pi^4Dh^2}F_i,(i=1,2),\\&\bar{p}=\frac{b^2}{\pi^2D}p,\ \bar{\Omega}_k=\frac{ab}{\pi^2}\left(\frac{\rho h}{D}\right)^{1/2}\ \Omega_k(k=1,2),\\&\varepsilon=\frac{12(1-\nu^2)h^2}{ab},\ \bar{t}=\frac{\pi^2}{ab}\left(\frac{D}{\rho h}\right)^{1/2}t,\\&\bar{\mu}=\frac{a^2b^2}{\pi^2h^4}\left(\frac{1}{12(1-\nu^2)\rho E}\right)^{1/2}\mu.\end{aligned} \tag{10}$$

where, ε is a small parameter. For simplicity, we drop the overbars in the following study. By means of Galerkin's method, the dimensionless equation of motion for the thin plate in the first two modes can be presented as follows

$$\begin{aligned}&\ddot{x}+\omega_1^2x+\varepsilon\mu\dot{x}+\varepsilon(\alpha_1x^3+\alpha_2xy^2)+2\varepsilon xf_1\cos\Omega_2t\\&=\varepsilon F_1\cos\Omega_1t\end{aligned} \tag{11}$$

$$\begin{aligned}&\ddot{y}+\omega_2^2y+\varepsilon\mu\dot{y}+\varepsilon(\beta_1y^3+\beta_2yx^2)+2\varepsilon yf_2\cos\Omega_2t\\&=\varepsilon F_2\cos\Omega_1t\end{aligned} \tag{12}$$

where,

$$\begin{aligned}&\alpha_1=\frac{\lambda^2+81}{16\lambda^2},\beta_1=\frac{1}{16}(81\lambda^2+\frac{1}{\lambda^2}),\\&\alpha_2=\beta_2=\frac{17\lambda^2}{(1+\lambda^2)^2}+\frac{625\lambda^2}{16(4+\lambda^2)^2}\\&\quad+\frac{625\lambda^2}{16(1+4\lambda^2)^2},\\&\omega_k^2=\left((\omega_k^*)^2-h_kp_0\right),\ h_k=\begin{cases}1, & k=1,\\9, & k=2,\end{cases}\\&p_1^*=(\omega_1^*)^2=\frac{(9+\lambda^2)^2}{\lambda^2},p_2^*=(\omega_2^*)^2=\frac{(9\lambda^2+1)^2}{\lambda^2},\\&f_k=\frac{1}{2}h_kp_1,k=1,2\end{aligned} \tag{13}$$

where, $\omega_{1,2}$ are the two linear natural frequencies of the thin-plate , λ is the aspect ratio of the plate, $p_{1,2}^*$ are the critical forces corresponding to two buckling modes at which thin plate loses its stability , $\omega_{1,2}^*$ are the natural frequencies of the two buckling modes and $f_{1,2}$ are the amplitudes of

parametric excitation.

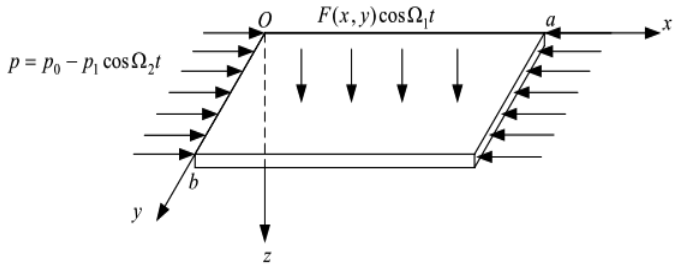

Fig. 1a. The rectangular thin plate model and its coordinate system.

From the system (Hegazy, 2010), we modified the equations of motion of the thin plate by adding the time delay of a linear velocity feedback as the following:

$$\ddot{x} + \omega_1^2 x + \varepsilon\mu\dot{x} + \varepsilon(\alpha_1 x^3 + \alpha_2 x y^2) + 2\varepsilon x f_1 \cos(\Omega_2 t) = \varepsilon F_1 \sum_{s=1}^{3} \frac{\cos(s\Omega_1 t)}{s} - \varepsilon G_1 \dot{x}(t-\tau) \tag{14}$$

$$\ddot{y} + \omega_2^2 y + \varepsilon\mu\dot{y} + \varepsilon(\beta_1 y^3 + \beta_2 y x^2) + 2\varepsilon y f_2 \cos(\Omega_2 t) = \varepsilon F_2 \sum_{s=1}^{3} \frac{\cos(s\Omega_1 t)}{s} - \varepsilon G_2 \dot{y}(t-\tau) \tag{15}$$

The main system is excited under parametric and multi-external excitation forces. The amplitudes of two modes of the system are x and y, time delay of a linear velocity feedback control is defined as τ which is added to the system, the thin plate natural frequencies are ω_1 and ω_2, the parameter of damping is μ, f_1 and f_2 are the in-plane forcing excitation, F_1 and F_2 are the transverse forcing excitation, Ω_1 and Ω_2 are the excitation frequencies, $\alpha_1, \alpha_2, \beta_1$ and β_2 are the non-linear parameters, G_1 and G_2 are feedback gains, ε is the parameter of perturbation and $0 < \varepsilon < 1$. A block diagram under time-delay feedback control describes the equations (14) and (15) as shown in Fig.1b.

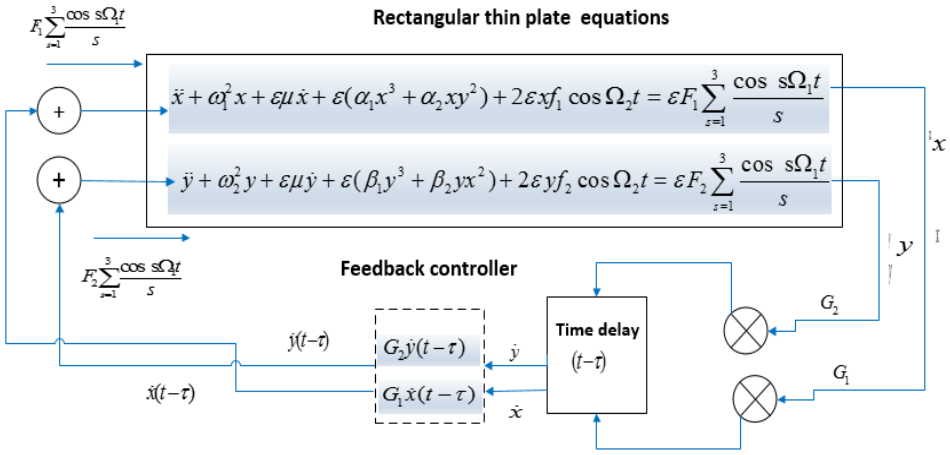

Fig. 1b. A block diagram for the model.

3. PERTURBATION ANALYSIS

Perturbation theory is a large group of mathematical methods applied to get the approximate solution to problems that have no closed-form analytical solution. These problems are a common happening in all branches of applied mathematics and engineering and found in different fields such as solid mechanics, fluid dynamics, quantum mechanics, optimal control, chemical reactor theory, aerodynamics, reaction-diffusion processes, and geophysics (Kumar, 2011). The methods operate by reducing a difficult problem to an infinite sequence of relatively easy problems that can be determined analytically and one of these methods is time-scale technique (Cai et al., 2017; Lizarraga et al., 2020).

The analytical solution of equations (14) and (15) up to the first-order approximation is obtained by the multiple time scales method (Nayfeh and Mook, 1979; Nayfeh, 1981) as in the form

$$x(t;\varepsilon) = x_0(T_0, T_1) + \varepsilon x_1(T_0, T_1) + O(\varepsilon^2) \tag{16a}$$

$$x(t-\tau;\varepsilon) = x_{0\tau}(T_0, T_1) + \varepsilon x_{1\tau}(T_0, T_1) + O(\varepsilon^2) \tag{16b}$$

$$y(t;\varepsilon) = y_0(T_0, T_1) + \varepsilon y_1(T_0, T_1) + O(\varepsilon^2) \tag{17a}$$

$$y(t-\tau;\varepsilon) = y_{0\tau}(T_0, T_1) + \varepsilon y_{1\tau}(T_0, T_1) + O(\varepsilon^2) \tag{17b}$$

Since, $T_m = \varepsilon^m t$ and the derivatives $D_m = \dfrac{\partial}{\partial T_m}$, (m=0, 1)

and the forms of derivatives are

$$\frac{d}{dt} = D_0 + \varepsilon D_1 + \ldots \tag{18}$$

$$\frac{d^2}{dt^2} = D_0^2 + 2\varepsilon D_0 D_1 + \ldots \tag{19}$$

Putting equations (16)-(19) into equations (14) and (15), and comparing the coefficients of like powers of ε leads to

Order ε^{o}

$$(D_o^2+\omega_1^2)x_o=0 \tag{20}$$

$$(D_o^2+\omega_2^2)y_o=0 \tag{21}$$

Order ε^{1}

$$(D_o^2+\omega_1^2)x_1=F_1\sum_{s=1}^{3}\frac{\cos s\Omega_1 t}{s}-2D_oD_1x_o-\mu D_ox_o-\alpha_1x_o^3 -\alpha_2x_oy_o^2-2x_of_1\cos\Omega_2 t-G_1D_ox_{o\tau} \tag{22}$$

$$(D_o^2+\omega_2^2)y_1=F_2\sum_{s=1}^{3}\frac{\cos s\Omega_1 t}{s}-2D_oD_1y_o-\mu D_oy_o-\beta_1y_o^3 -\beta_2y_ox_o^2-2y_of_2\cos\Omega_2 t-G_2D_oy_{o\tau} \tag{23}$$

The General Solution of the equations (7) and (8), become

$$x_o(T_o,T_1)=A_o(T_1)e^{i\omega_1T_o}+cc \tag{24a}$$

$$y_o(T_o,T_1)=B_o(T_1)e^{i\omega_2T_o}+cc \tag{24b}$$

since, A_o and B_o indicate the complex functions in T_1 and cc are the complex conjugate terms. Using Taylor series (see Wirkus and Rand, 2002) for expanding $A_{o\tau}$ and $B_{o\tau}$, yields

$$A_{o\tau}(T_1)=A_{o\tau}(T_1-\varepsilon\tau)\cong A_o(T_1)-\varepsilon\tau A_o'(T_1)+... \tag{25a}$$

$$B_{o\tau}(T_1)=B_{o\tau}(T_1-\varepsilon\tau)\cong B_o(T_1)-\varepsilon\tau B_o'(T_1)+... \tag{25b}$$

Substituting equations (24) and (25) into equations (22) and (23), we obtain

$$\begin{aligned}(D_o^2+\omega_1^2)x_1 =&[-2i\omega_1(D_1A_o)-i\omega_1\mu A_o-3\alpha_1A_o^2\overline{A}_o\\ &-2\alpha_2A_oB_o\overline{B}_o-i\omega_1G_1A_oe^{-i\omega_1\tau}]e^{i\omega_1T_o}\\ &-\alpha_1A_o^3e^{3i\omega_1T_o}-\alpha_2A_oB_o^2e^{i(\omega_1+2\omega_2)T_o}\\ &-\alpha_2A_o\overline{B}_o^2e^{i(\omega_1-2\omega_2)T_o}+F_1\sum_{s=1}^{3}\frac{1}{2s}e^{is\Omega_1T_o}\\ &-f_1A_oe^{i(\Omega_2+\omega_1)T_o}-f_1\overline{A}_oe^{i(\Omega_2-\omega_1)T_o}+cc\end{aligned} \tag{26}$$

$$\begin{aligned}(D_o^2+\omega_2^2)y_1 =&[-2i\omega_2(D_1B_o)-i\mu\omega_2B_o-3\beta_1B_o^2\overline{B}_o\\ &-2\beta_2B_oA_o\overline{A}_o-i\omega_2G_2B_oe^{-i\omega_2\tau}]e^{i\omega_2T_o}\\ &-\beta_1B_o^3e^{3i\omega_2T_o}-\beta_2B_oA_o^2e^{i(\omega_2+2\omega_1)T_o}\\ &-\beta_2B_o\overline{A}_o^2e^{i(\omega_2-2\omega_1)T_o}+F_2\sum_{s=1}^{3}\frac{1}{2s}e^{is\Omega_1T_o}\\ &-f_2B_oe^{i(\Omega_2+\omega_2)To}-f_2\overline{B}_oe^{i(\Omega_2-\omega_2)To}+cc\end{aligned} \tag{27}$$

After, revoking the secular terms in equations (26) and (27) the solutions can be given as,

$$\begin{aligned}x_1(T_o,T_1)=&A_1e^{i\omega_1T_o}+C_1^*e^{3i\omega_1T_o}+C_2^*e^{i(\omega_1+2\omega_2)T_o}\\ &+C_3^*e^{i(\omega_1-2\omega_2)T_o}+C_4^*e^{is\Omega_1T_o}+C_5^*e^{i(\Omega_2+\omega_1)T_o}\\ &+C_6^*+cc\end{aligned} \tag{28}$$

$$\begin{aligned}y_1(T_o,T_1)=&B_1e^{i\omega_2T_o}+H_1^*e^{3i\omega_2T_o}+H_2^*e^{i(\omega_2+2\omega_1)T_o}\\ &+H_3^*e^{i(\omega_2-2\omega_1)T_o}+H_4^*e^{is\Omega_1T_o}+H_5^*e^{i(\Omega_2+\omega_2)T_o}\\ &+H_6^*e^{i(\Omega_2-\omega_2)T_o}+cc\end{aligned} \tag{29}$$

since, A_1 and B_1 indicate the complex functions in T_1 and cc are the complex conjugate terms. We can deduce all resonance cases from the above-determined solutions, which can be classified as:

(i) Primary Resonance: $\Omega_1\cong\omega_1,\Omega_1\cong\omega_2$.

(ii) Internal Resonance: $\omega_1\cong\omega_2$

(iii) Sub-harmonic Resonance: $\Omega_2\cong2\omega_1,\Omega_2\cong2\omega_2$.

(iv) Super- harmonic Resonance: $\Omega_1\cong m\omega_1$, $m=\frac{1}{2},\frac{1}{3}$.

(v) Simultaneous Resonance is any collection of the up resonance cases.

4. THE PERIODIC SOLUTION

At simultaneous worst resonance case ($\Omega_1=\omega_1=\omega_2$) we can study the stability by inserting the detuning parameters $\sigma_n(n=1,2)$ as follows,

$$\Omega_1\cong\omega_1+\varepsilon\sigma_1,\Omega_1\cong\omega_2+\varepsilon\sigma_2 \tag{30}$$

Substituting from equation (17) into equations (13) and (14), we get the condition of solvability,

$$\begin{aligned}&[-2i\omega_1DA_o-i\omega_1\mu A_o-3\alpha_1A_o^2\overline{A}_o-2\alpha_2A_oB_o\overline{B}_o\\ &-i\omega_1G_1A_oe^{-i\omega_1\tau}]+\frac{F_1}{2}e^{i\sigma_1T_1}-\alpha_2\overline{A}_oB_o^2e^{2i(\sigma_1-\sigma_2)T_1}=0\end{aligned} \tag{31}$$

$$\begin{aligned}&[-2i\omega_2DB_o-i\omega_2\mu B_o-3\beta_1B_o^2\overline{B}_o-2\beta_2B_oA_o\overline{A}_o\\ &-i\omega_2G_2B_oe^{-i\omega_2\tau}]+\frac{F_2}{2}e^{i\sigma_2T_1}-\beta_2\overline{B}_oA_o^2e^{-2i(\sigma_1-\sigma_2)T_1}=0\end{aligned} \tag{32}$$

Using the polar form,

$$A_o=\frac{a_1}{2}e^{i\gamma_1}\quad and\quad B_o=\frac{a_2}{2}e^{i\gamma_2} \tag{33}$$

where, $a_i (i = 1,2)$ are amplitudes of the steady-state and $\gamma_i (i = 1,2)$ are the motions phases. From equation (20) into equations (31) and (32), and resolve imaginary and real parts, yields

$$\dot{a}_1 = -\frac{\mu}{2} a_1 - \frac{G_1}{2} a_1 \cos(\omega_1 \tau) + \frac{F_1}{2\omega_1} \sin\psi_1 - \frac{\alpha_2}{8\omega_1} a_1 a_2^2 \sin 2\psi \quad (34)$$

$$a_1 \dot{\gamma}_1 = \frac{3\alpha_1}{8\omega_1} a_1^3 + \frac{\alpha_2}{4\omega_1} a_1 a_2^2 + \frac{G_1}{2} a_1 \sin(\omega_1 \tau) - \frac{F_1}{2\omega_1} \cos\psi_1 + \frac{\alpha_2}{8\omega_1} a_1 a_2^2 \cos 2\psi \quad (35)$$

$$\dot{a}_2 = -\frac{\mu}{2} a_2 - \frac{G_2}{2} a_2 \cos(\omega_2 \tau) + \frac{F_2}{2\omega_2} \sin\psi_2 + \frac{\beta_2}{8\omega_2} a_2 a_1^2 \sin 2\psi \quad (36)$$

$$a_2 \dot{\gamma}_2 = \frac{3\beta_1}{8\omega_2} a_2^3 + \frac{\beta_2}{4\omega_2} a_2 a_1^2 + \frac{G_2}{2} a_2 \sin(\omega_2 \tau) - \frac{F_2}{2\omega_2} \cos\psi_2 + \frac{\beta_2}{8\omega_2} a_2 a_1^2 \cos 2\psi \quad (37)$$

where, $\psi_1 = (\sigma_1 T_1 - \gamma_1), \psi_2 = (\sigma_2 T_1 - \gamma_2)$ and

$$\psi = (\sigma_1 - \sigma_2) T_1 - \gamma_1 + \gamma_2 .$$

4.1 Stability of Fixed Points

For steady-state solutions, $\dot{a}_m, \dot{\psi}_m = 0,\ m = 1,2$ and fixed points of the above equations (34)-(37) are given by,

$$-\frac{\mu}{2} a_1 - \frac{G_1}{2} a_1 \cos(\omega_1 \tau) + \frac{F_1}{2\omega_1} \sin\psi_1 - \frac{\alpha_2}{8\omega_1} a_1 a_2^2 \sin 2\psi = 0 \quad (38)$$

$$a_1 \sigma_1 - \frac{3\alpha_1}{8\omega_1} a_1^3 - \frac{\alpha_2}{4\omega_1} a_1 a_2^2 - \frac{G_1}{2} a_1 \sin(\omega_1 \tau) + \frac{F_1}{2\omega_1} \cos\psi_1 - \frac{\alpha_2}{8\omega_1} a_1 a_2^2 \cos 2\psi = 0 \quad (39)$$

$$-\frac{\mu}{2} a_2 - \frac{G_2}{2} a_2 \cos(\omega_2 \tau) + \frac{F_2}{2\omega_2} \sin\psi_2 + \frac{\beta_2}{8\omega_2} a_2 a_1^2 \sin 2\psi = 0 \quad (40)$$

$$a_2 \sigma_2 - \frac{3\beta_1}{8\omega_2} a_2^3 - \frac{\beta_2}{4\omega_2} a_2 a_1^2 - \frac{G_2}{2} a_2 \sin(\omega_2 \tau) + \frac{F_2}{2\omega_2} \cos\psi_2 - \frac{\beta_2}{8\omega_2} a_2 a_1^2 \cos 2\psi = 0 \quad (41)$$

Then the steady-state solutions of a rectangular thin plate are obtained numerically by using (package fsolve in Matlab R2014a).

4.2 The Linear Solution Analysis

For determining the stability of the linear solution of equations (31) and (32), we introduce the following forms: Let A_o and B_o Expressed in Cartesian as:

$$A_o(T_1) = \frac{1}{2}(p_1 - iq_1) e^{i\sigma_1 T_1} \text{ and } B_o(T_1) = \frac{1}{2}(p_2 - iq_2) e^{i\sigma_2 T_1} \quad (42)$$

Where, p_n and q_n , $n = 1,2$ are real values. Substituting the above forms of A_o and B_o into the linearized form of equations (31) and (32), we get

$$-2i\omega_1 A_o' - i\omega_1 \mu A_o - i\omega_1 G_1 A_o e^{-i\omega_1 \tau} = 0 \quad (43)$$

$$-2i\omega_2 B_o' - i\omega_2 \mu B_o - i\omega_2 G_2 B_o e^{-i\omega_2 \tau} = 0 \quad (44)$$

Substituting equation (42) into equations (43) and (44) and by making a comparison between imaginary and real parts, then we obtain the following system of equations.

$$p_1' = -Q_1 p_1 - Q_2 q_1 \quad (45)$$

$$q_1' = -Q_1 q_1 + Q_2 p_1 \quad (46)$$

$$p_2' = -Q_3 p_2 - Q_4 q_2 \quad (47)$$

$$q_2' = -Q_3 q_2 + Q_4 p_2 \quad (48)$$

For the linear solution, the conditions of the stability are obtained from zero characteristic equation.

$$\begin{vmatrix} \lambda + Q_1 & Q_2 & 0 & 0 \\ -Q_2 & \lambda + Q_1 & 0 & 0 \\ 0 & 0 & \lambda + Q_3 & Q_4 \\ 0 & 0 & -Q_4 & \lambda + Q_3 \end{vmatrix} = 0 \quad (49)$$

The Eigen values are given by

$$\lambda = -Q_1 \pm iQ_2,$$

$$\lambda = -Q_3 \pm iQ_4$$

The linear solution is stable if and only if $Q_1, Q_3 > 0$, otherwise is unstable.

4.3 Stability for a nonlinear solution

The stability for a non-linear solution can be calculated as follows

Let, $a_m = a_{m0} + a_{m1}, \psi_m = \psi_{m0} + \psi_{m1}, m = 1,2$ (50)

Since a_{m0} and ψ_{m0} verify equations (38)-(41) and a_{m1}, ψ_{m1} are small approximation comparing with a_{m0} and ψ_{m0}. Substituting from equation (50) into equations (34)-(37), we get

$$\dot{a}_{11} = \delta_1 a_{11} + \delta_2 \psi_{11} + \delta_3 \psi_{21} \tag{51}$$

$$\dot{\psi}_{11} = \delta_4 a_{11} + \delta_5 \psi_{11} + \delta_6 a_{21} + \delta_7 \psi_{21} \tag{52}$$

$$\dot{a}_{21} = \delta_8 \psi_{11} + \delta_9 a_{21} + \delta_{10} \psi_{21} \tag{53}$$

$$\dot{\psi}_{21} = \delta_{11} a_{11} + \delta_{12} \psi_{11} + \delta_{13} a_{21} + \delta_{14} \psi_{21} \tag{54}$$

The equations (51)-(54) can be written as follows,

$$\left[\dot{a}_{11} \;\; \dot{\psi}_{11} \;\; \dot{a}_{21} \;\; \dot{\psi}_{21}\right]^T = [J]\left[a_{11} \;\; \psi_{11} \;\; a_{21} \;\; \psi_{21}\right]^T \tag{55}$$

where $[J]$ is the Jacobin matrix of these equations and defined as

$$[J] = \begin{bmatrix} \delta_1 & \delta_2 & 0 & \delta_3 \\ \delta_4 & \delta_5 & \delta_6 & \delta_7 \\ 0 & \delta_8 & \delta_9 & \delta_{10} \\ \delta_{11} & \delta_{12} & \delta_{13} & \delta_{14} \end{bmatrix} \tag{56}$$

Where δ_i, (i=1, 2, ..., 14) are the coefficients which are defined in Appendix. The Eigen values can be given from the characteristic equation

$$\begin{vmatrix} \delta_1 - \lambda & \delta_2 & 0 & \delta_3 \\ \delta_4 & \delta_5 - \lambda & \delta_6 & \delta_7 \\ 0 & \delta_8 & \delta_9 - \lambda & \delta_{10} \\ \delta_{11} & \delta_{12} & \delta_{13} & \delta_{14} - \lambda \end{vmatrix} = 0 \tag{57}$$

$$\lambda^4 + r_1\lambda^3 + r_2\lambda^2 + r_3\lambda + r_4 = 0 \tag{58}$$

where, $r_i (i = 1, 2, 3, 4)$ are the coefficients of equation (44) and given in the appendix. . According to the criterion of the Routh-Hurwitz, the stability of the periodic solution is satisfied if the real parts of all eigenvalues of Jacobin equation (57) are less than zero otherwise be unstable and investigated as follows.

$$r_1 > 0, r_1 r_2 - r_3 > 0, r_3(r_1 r_2 - r_3) - r_1^2 r_4 > 0, r_4 > 0$$

5. RESULTS AND DISCUSSION

In this section, the Runge-Kutta fourth-order (RK-4) method (package ode45) is applied to get the numerical solution for the differential equations (14) and (15) of the rectangular thin plate with time delay feedback at the simultaneous internal and primary resonance case $(\Omega_1 = \omega_1 = \omega_2)$. Fig. 2 shows the response of the non-resonant system, where the steady-state amplitudes (x) and (y) are about (0.085) and (0.023), respectively, this case can be considered as a basic case at chosen values of the equation parameters from (as given in Bauomy and El-Sayed, 2016).

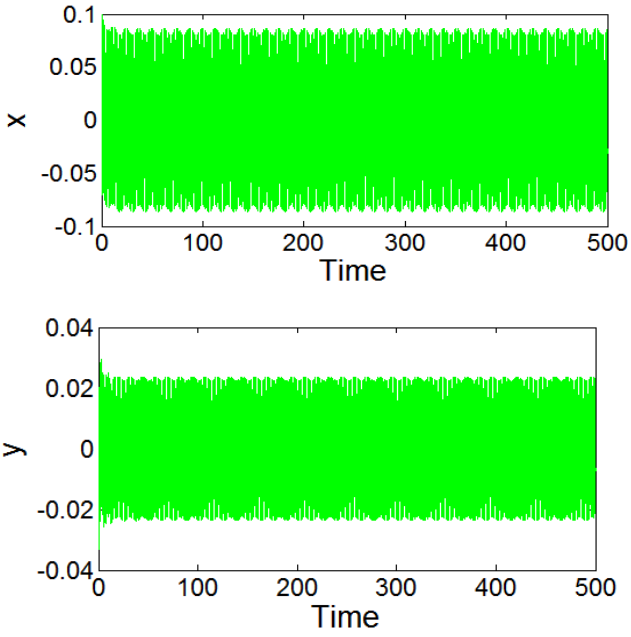

Fig. 2. Non resonant case for the system.

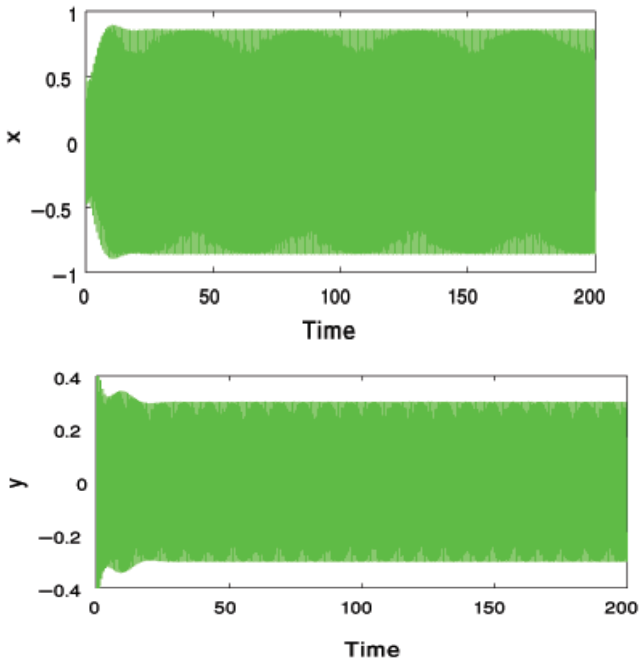

Fig. 3. Simultaneous internal and primary resonances case without control.

$$(\omega_1 = 8, \omega_2 = 9, \alpha_1 = 5.125, \alpha_2 = 7.375, \beta_1 = 5.125, \beta_2 = 7.375,$$

$$\Omega_1 = 4, \Omega_2 = 4.5, F_1 = 4, F_2 = 1.5, f_1 = 0.4, f_2 = 0.25, \mu = 0.4).$$

For the simultaneous internal and primary resonances case $(\Omega_1 = \omega_1 = \omega_2)$ as appeared in Fig. 3, the vibration amplitudes of the system are increased to about (0.85) with

an increasing rate 1000% for (x) and to about (0.3) with an increasing rate 1300 % for (y)of their comparable values presented in Fig. 2. From Fig. 4. the time delay feedback is applied to the worst resonances case, where $(\Omega_1 = \omega_1 = \omega_2)$. We noticed that the vibration amplitudes of the system are decreased to about (0.048) with a reduction rate 94.4% for (x) and to about (0.025) with a reduction rate 92% for (y). This indicates the effectiveness of the time delay feedback ($E_a = 18$ and $E_a = 12$ for (x) and (y), respectively)

(E_a = the steady-state amplitude of the main system before the controller/ the steady-state amplitude of the main system after the control).

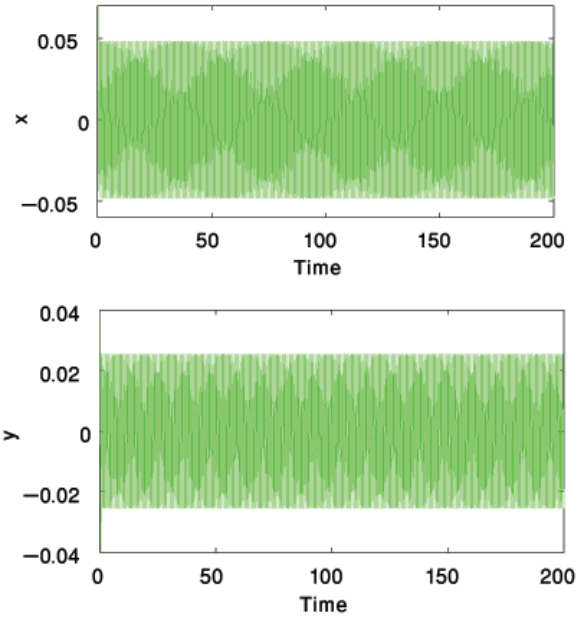

Fig. 4. Simultaneous internal and primary resonances case.

with time delay feedback $\tau = 0.05$

In figure 5, the effect of gains (G_1 and G_2) and the nonlinear parameters (α_1, α_2, β_1 and β_2) of the main system for two modes (x) and (y), respectively are studied numerically without control. From Fig. 5a and 5b, we noticed that more increases in gains lead to monotonic decrease in the system amplitudes and cause saturation phenomena. Also, the increase in the nonlinear parameters leads to monotonic decrease in the steady-state amplitudes on the main system for two modes (x) and (y) as shown in Figs. (5c) - (5f). In

Fig. 6. the response of the system via time delay feedback was studied numerically. It is noticed that, the vibration amplitudes of the system can be suppressed at some values of the time delay as in the rang ($0.01 \le \tau \le 0.13$) for (x) and in the range ($0.01 \le \tau \le 0.11$) for (y). This region called "safe region for vibration" After this range, the response of the system is increasing and decreasing.

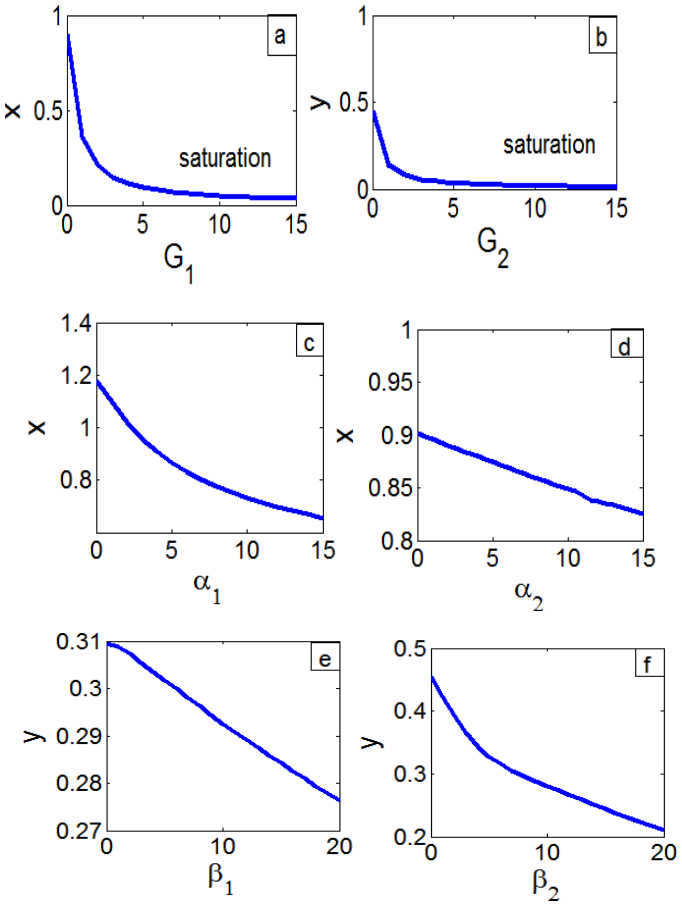

Fig. 5. The effect of gains and the nonlinear parameters of the main system without delay.

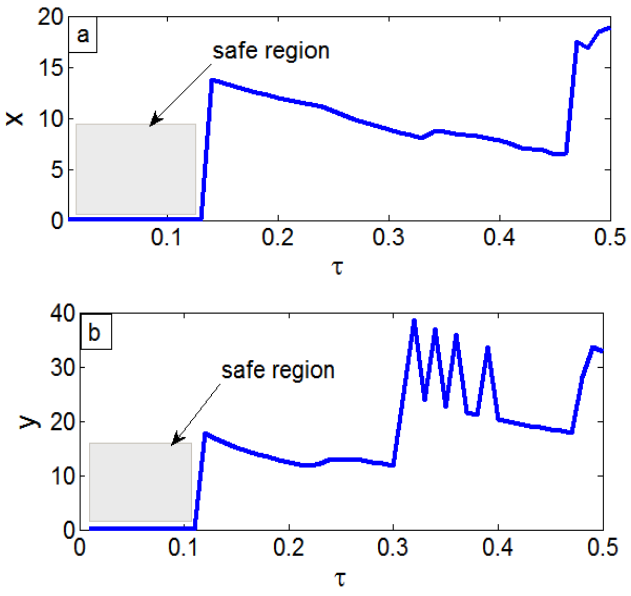

Fig. 6. The behavior of the system via time-delay feedback.

5.1 Frequency response curves

The second part of this section is to study the influence of parameters on the steady-state amplitudes of the main system with time delay feedback from the frequency response equations as presented in Eqs. (38)- (41) at ($a_1 \neq 0$, $a_2 \neq 0$).

From Figs. 7a and 7b show the behavior of the external excitation forces F_1 and F_2 for different values on the uncontrolled system. It is noticed that the increase in the transverse forcing excitation F_1 and F_2 leads to monotonic increase in the steady-state amplitudes a_1 and a_2, respectively, and unstable regions appears as shown in Fig. 7a. Hence, the system will be destroyed by increasing the excitation forces so the system must be controlled.

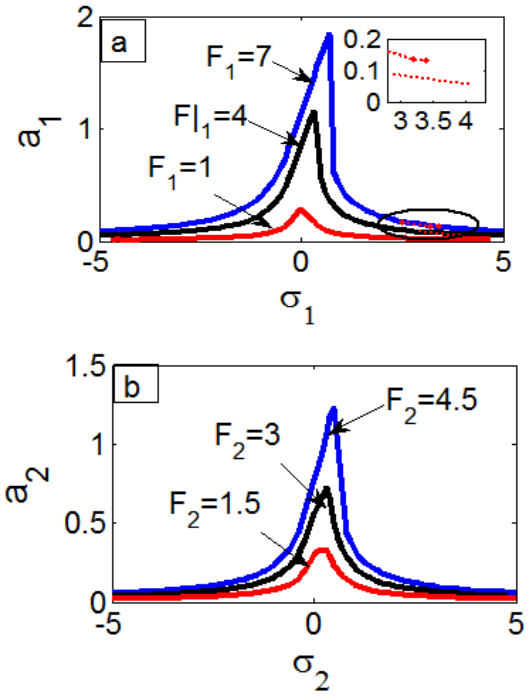

Fig. 7. The effect of the external excitations F_1 and F_2 on the uncontrolled system.

Fig. 8a represents the basic case on frequency response curve a_1 against σ_1 after adding time delay. Fig. 8b displays the curves of the frequency response of the external excitation force F_1 for different values on the controlled system. It is noticed that the steady- state amplitude a_1 of the system is increased when the excitation force F_1 increased. Figs. 8c, 8d and 8e show steady-state amplitude of the system response a_1 is monotonic decreasing for increasing the values of the natural linear frequency ω_1, the damping linear coefficient μ and the gain G_1.

Fig. 9a is considered as a basic case on the frequency response curve a_2 against σ_2 for controlled system. Fig. 9b clear that the steady-state amplitude a_2 of the system is monotonic increasing when the values of the excitation force F_2 increased. Figs. 9c, 9d and 9e show the steady-state amplitude a_2 of the system response is monotonic decreasing when the values of the natural linear frequency ω_2, the damping linear coefficient μ and the gain G_1 are increasing. Fig. 10. illustrate the effects of increases the nonlinear parameters α_1, α_2, β_1 and β_2 via time delay feedback. From this figure, it is noticed that the system amplitudes may be increased or decreased but this effect doesn't appear clearly because these values are very small. For instance, the system amplitude (x) ranges from 0.0481995 to 0.0481999 as shown in Figs. 10a and 10b and for the system amplitude (y) ranges from 0.0253359 to 0.0253373 as shown in Figs. 10c and 10d.

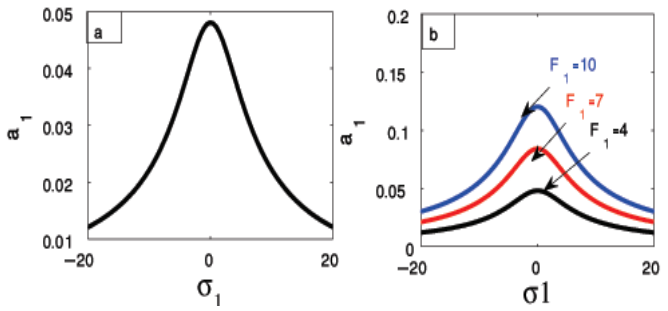

(a) Frequency response curve a_1 against σ_1, (b) The effect of external force F_1

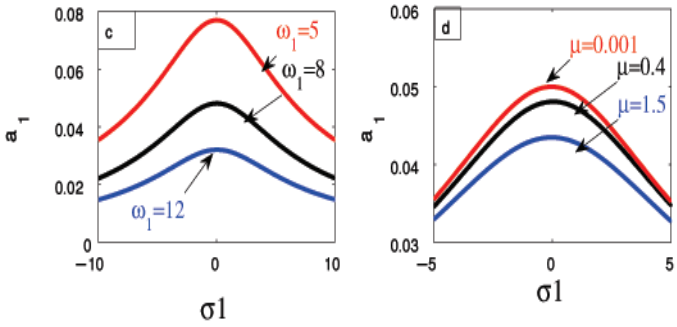

(c) The effect of natural frequency ω_1, (d) The effect of damping coefficient μ

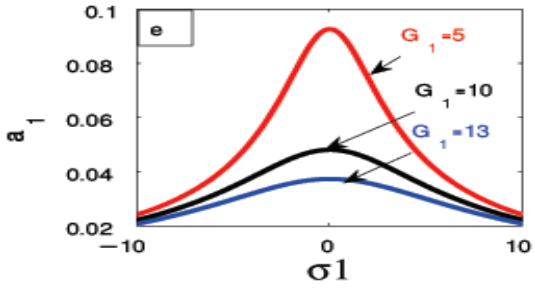

(e) The effect of Gain G_1

Fig. 8. Frequency response curves for the steady-state amplitude a_1 at different parameters under controlled system.

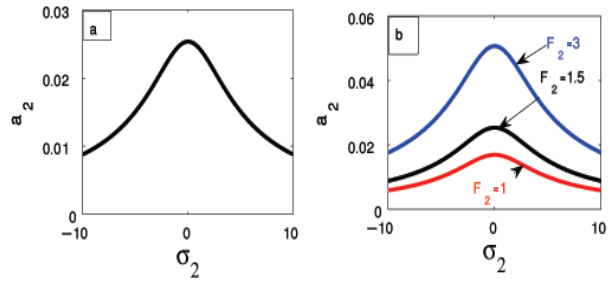

(a) Frequency response curve a_2 against σ_2, (b) The effect of external force F_2

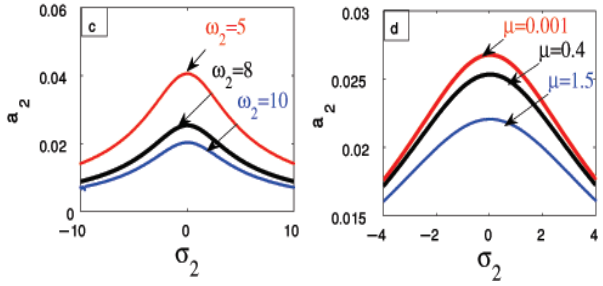

(c) The effect of natural frequency ω_2, (d) The effect of damping coefficient μ

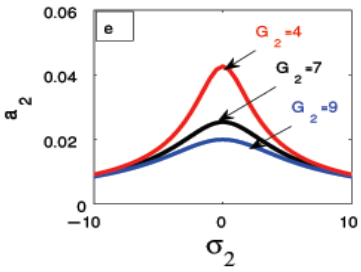

(e) The effect of Gain G_2

Fig. 9 Frequency response curves for the steady-state amplitude a_2 at different parameters under controlled system

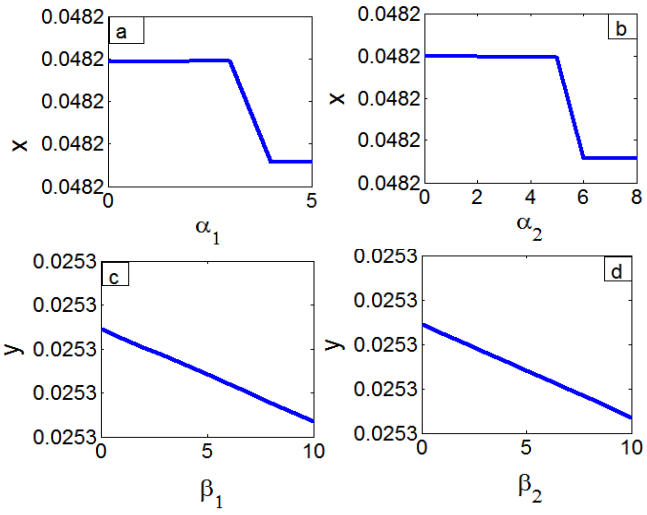

Fig. 10. The outcomes of the nonlinear parameters under a controlled system.

5.2 Agreements between the outcomes (Numerical solution, Analytical solution and Frequency response curves)

From Fig. 11 there is a validation between the numerical solution of equations (14) and (15) by (RK-4) method and the approximate solution given by equations (34)-(37) using the multiple-scale perturbation method at the worst resonance case $(\Omega_1 = \omega_1 = \omega_2)$ when $\sigma_1 = \sigma_2 = 0$. For the frequency response curves of the steady- state amplitudes a_1 and a_2, there is a good agreement between the frequency response solutions deduced from the equations (34)-(37) (indicated as a blue solid line) and numerical solution given by (RK-4) method(indicated as red small circles) as shown in Fig. 12.

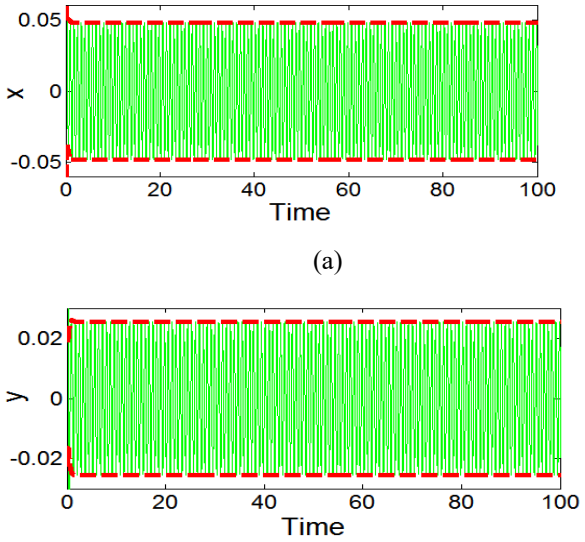

(Numerical solution, Perturbation solution)

Fig. 11. Comparsion between the analytical and the numerical solutions.

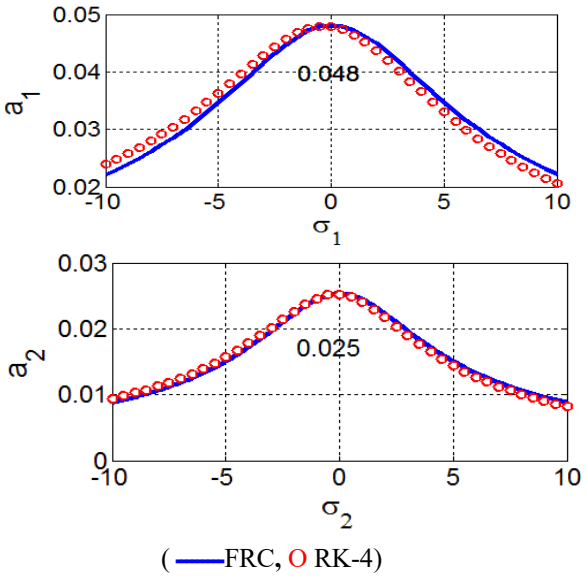

(FRC, O RK-4)

Fig. 12. Comparison between the solutions of frequency response and (RK-4) method.

6. COMPARISON WITH THE PREVIOUSLY PUBLISHED WORK

1. Hegazy, 2010 analyzed the chaotic motion and the dynamic performance of rectangular thin-plate under both external and parametric excitation forces without adding any control. The stability analysis is investigated and studied at the worst resonance case that is simultaneously internal and primary resonance case $(\Omega_1 = \omega_1 = \omega_2)$ by using frequency response equations and phase plane techniques.

2. in this paper,

The dynamic behavior of the thin-plate is analyzed by making a comparison between three negative active controllers (Acceleration feedback control, Cubic velocity feedback control, and linear velocity time delay feedback control) to the worst resonance case $(\Omega_1 = \omega_1 = \omega_2)$ as shown in Fig. 13. We noticed that the amplitudes of the system extremely decrease the vibration in the time delay feedback controller and also in the other controllers. The best effectiveness of the system is achieved with in the time delay feedback controller (see table 1).

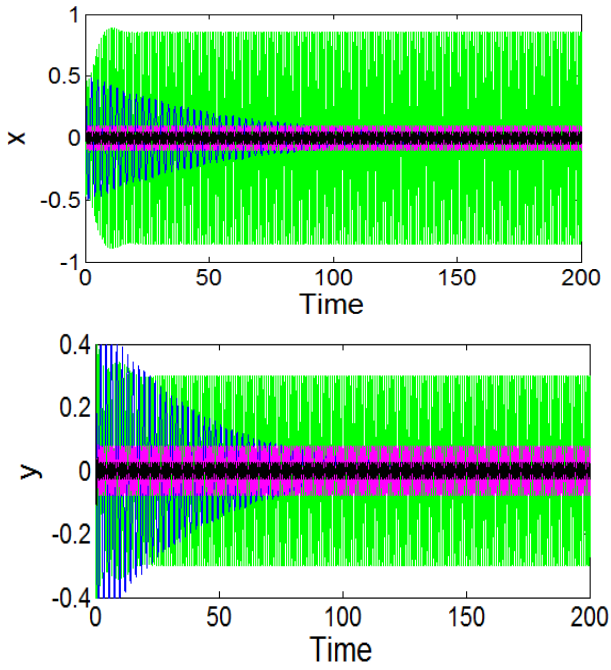

Fig. 13. Comparison between three different types of controls.

(——— The worst resonance case, ——Acceleration feedback control, ——— Cubic velocity feedback, ——the time delay of a linear velocity feedback)

So, we succeeded in suppressing the vibrations directly from t=0 (second) after adding the time-delay feedback control at the mentioned worst resonance as shown in Fig.4. Finally, experimental results exhibited that the time delay feedback is more suitable for the controlling speed and reduced the dynamic vibration.

Table 1. Comparison between three different types of controls.

Type of feedback controller	Amplitude with controller		Time(s)		E_a (times)	
	x	y	x	y	x	y
1. Acceleration	0.08	0.03	t=100	t=100	11	10
2. Cubic	0.09	0.07	t=0	t=0	9	4
3. Time delay	0.048	0.025	t=0	t=0	18	12

7. CONCLUSIONS

The time delay feedback control was added to decrease the high amplitudes of a thin-plate at the considered resonance .The analytical solution up to first-order approximation is obtained by using the method of multiple scales. We succeed in reducing the vibrations of the thin plate for two modes (x) and (y) of the system. Then from the above numerical study, the outcomes can be declared as follows.

1. The worst resonance case $(\Omega_1 = \omega_1 = \omega_2)$ caused the highest vibrations for a rectangular thin plate to be about (0.85) for the first mode (x) and (0.3) for the second mode (y).

2. The steady-state amplitudes are decreased to (0.048) for x and (0.025) for (y) after adding time-delay feedback control compared with the steady-state amplitudes of the system without the controller.

3. The controller is effectiveness, E_a = 18 and E_a =12 for the system amplitudes (x) and (y), respectively.

4. The amplitudes of the main system are decreased in the range ($0.01 \le \tau \le 0.13$) and ($0.01 \le \tau \le 0.11$) for two modes (x) and (y), respectively.

5. Increasing the transversal forcing excitation F_1 and F_1 lead to an increase in the amplitudes of the main system.

6. Increasing the values of the natural frequencies ω_1 , ω_2 and the damping coefficient μ lead to a monotonic decrease in the steady-state amplitudes of the system.

7. The steady-state amplitudes of the system is shifted to the down and decreased by increasing the values of Gains G_1 and G_2 .

8. All predictions deduced from the approximate solutions are in good agreement with the numerical analysis as shown in Figs. 11, 12.

REFERENCES

Amer, Y., El-Sayed, A., and Kotb, A. (2016). Nonlinear vibration and of the duffing oscillator to parametric excitation with time delay feedback. *Nonlinear Dynamics,* 85 (4), 2497-2505.

Bauomy, H. S., and El-Sayed, A. T. (2016). Active control of a rectangular thin plate via negative acceleration feedback. *Journal of Computational and Nonlinear Dynamics,* 11(4).

Cai, C., Wang, Z., Xu, J., and Zou, Y. (2017). Singular Perturbation Methods and Time-Scale Techniques. In finite frequency analysis and synthesis for singularly perturbed systems .*Springer*, Cham, 3-27.

El-Bassiouny, A. (2006). Stability and oscillation of two coupled duffing equations with time delay state feedback. *Physica Scripta*, 74 (6),726-735.

El-Ganaini, W., and ElGohary, H. (2011). Vibration suppression via time-delay absorber described by non-linear differential equations. *Adv. Theor. Appl. Mech*, 4 (2),49-67.

El-Gohary, H., and El-Ganaini, W. (2012). Vibration suppression of a dynamical system to multi-parametric excitations via time-delay absorber. *Applied Mathematical Modelling*, 36 (1), 35-45.

El-Sayed, A., and Bauomy, H. (2014).Vibration control of helicopter blade flapping via time-delay absorber. *Meccanica*, 49(3), 587-600.

Gouskov, A. M., Voronov, S. A., Paris, H., and Batzer, S. A. (2002). Nonlinear dynamics of a machining system with two interdependent delays. Communications in *Nonlinear Science and Numerical Simulation*, 7 (4), 207-221.

Guo, X., and Zhang, W. (2011). Nonlinear dynamics of composite laminated thin plate with 1 2 3 inner resonance. *Second International Conference on Mechanic Automation and Control Engineering*, IEEE, 7479- 7482.

Hegazy, U. H. (2010). Nonlinear vibrations of a thin plate under simultaneous internal and external resonances. *Journal of vibration and acoustics*, 132 (5).

Kumar, M. (2011). Methods for solving singular perturbation problems arising in science and engineering. *Mathematical and Computer Modelling*, 54(1-2), 556-575.

Kim, C. H., Lee, C.W., and Perkins, N. (2005). Nonlinear vibration of sheet metal plates under interacting parametric and external excitation during manufacturing. *J. Vib. Acoust*., 127 (1), 36(43).

Lai, S. K., Lim, C. W., Xiang, Y., and Zhang, W. (2009). On asymptotic analysis for large amplitude nonlinear free vibration of simply supported laminated plates, *Journal of vibration and acoustics*, 131 (5).

Lu, W., and Liu, Y. (2009).Vibration control for the primary resonance of the duffing oscillator by a time delay state feedback. *Int. J. Nonlinear Sci*, 8 (3), 324-328.

Lizarraga, I., Rink, B., and Wechselberger, M. (2020). Multiple timescales and the parametrisation method in geometric singular perturbation theory. *arXiv preprint arXiv:* 2009.10583.

Nayfeh, A. H . (1981). Perturbation Techniques. *New York: Wiley.*

Nayfeh, A. H., and Mook, D. (1979). Nonlinear Oscillations. *New York: Wiley*.

Saeed, N., El-Ganini, W., and Eissa, M. (2013). Nonlinear time delay saturation-based controller for suppression of nonlinear beam vibrations. *Applied Mathematical Modelling* 37 (20-21) (2013) 8846-8864.

Sayed, M., and Mousa, A. (2012). Second-order approximation of angle-ply composite laminated thin plate under combined excitations. *Communications in Non- linear Science and Numerical Simulation,* 17 (12), 5201-5216.

Wirkus, S., and Rand, R. (2002). The dynamics of two coupled van der pol oscillators with delay coupling. *Nonlinear dynamics,* 30 (3), 205-221.

Zhang, W. (2001). Global and chaotic dynamics for a parametrically excited thin plate. *Journal of Sound and Vibration,* 239 (5), 1013-1036.

Zhang, W., and Li, S. (2010). Resonant chaotic motions of a buckled rectangular thin plate with parametrically and externally excitations. *Nonlinear Dynamics*, 62 (3), 673-686.

Zhang, W., Liu, Z., and Yu, P. (2001). Global dynamics of a parametrically and externally excited thin plate. *Nonlinear Dynamics,* 24 (3), 245-268.

Zhao, Y., and Xu, J. (2007). Effects of delayed feedback control on nonlinear vibration absorber system. *Journal of Sound and Vibration,* 308 (1-2), 212-230.

APPENDIX

Coefficients of equation (28)

$$C_1^* = \frac{\alpha_1 A_o^3}{8\omega_1^2}, C_2^* = -\frac{\alpha_2 A_o B_o^2}{\omega_1^2 - (\omega_1 + 2\omega_2)^2},$$

$$C_3^* = \frac{\alpha_2 A_o \overline{B}_o^2}{\omega_1^2 - (\omega_1 - 2\omega_2)^2}, C_4^* = \frac{F_1}{2}\sum_{s=1}^{3}\frac{1}{s(\omega_1^2 - (s\Omega_1)^2)},$$

$$C_5^* = -\frac{f_1 A_o}{\omega_1^2 - (\omega_1 + \Omega_2)^2}, C_6^* = \frac{f_1 \overline{A}_o}{\omega_1^2 - (\Omega_2 - \omega_1)^2}$$

Coefficients of equation (29)

$$H_1^* = \frac{\beta_1 B_o^3}{8\omega_2^2}, H_2^* = -\frac{\beta_2 B_o A_o^2}{\omega_2^2 - (\omega_2 + 2\omega_1)^2}$$

$$H_3^* = \frac{\beta_2 B_o \overline{A}_o^2}{\omega_2^2 - (\omega_2 - 2\omega_1)^2}, H_4^* = \frac{F_2}{2}\sum_{s=1}^{3}\frac{1}{s(\omega_2^2 - (s\Omega_1)^2)}$$

$$H_5^* = -\frac{f_2 B_o}{\omega_2^2 - (\Omega_2 + \omega_2)^2}, H_6^* = \frac{f_2 \overline{B}_o}{\omega_2^2 - (\Omega_2 - \omega_2)^2}$$

Coefficients of system of equations (25)-(48)

$$Q_1 = (\frac{\mu}{2} + \frac{G_1}{2}\cos\omega_1\tau), Q_2 = (\sigma_1 - \frac{G_1}{2}\sin\omega_1\tau),$$

$$Q_3 = (\frac{\mu}{2} + \frac{G_2}{2}\cos\omega_2\tau), Q_4 = (\sigma_2 - \frac{G_2}{2}\sin\omega_2\tau)$$

Coefficients of system of equations (51)-(54)

$$\delta_1 = (-\frac{1}{2}\mu - \frac{1}{2}G_1\cos\omega_1\tau),$$

$$\delta_2 = (\frac{F_1}{2\omega_1}\cos\psi_{10} - \frac{2\alpha_2}{8\omega_1}a_{10}a_{20}^2(\cos 2\psi_{10}\cos 2\psi_{20} + \sin 2\psi_{10}\sin 2\psi_{20})),$$

$$\delta_3 = (\frac{2\alpha_2}{8\omega_1}a_{10}a_{20}^2(\sin 2\psi_{10}\sin 2\psi_{20} + \cos 2\psi_{10}\cos 2\psi_{20}),$$

$$\delta_4 = (\frac{\sigma_1}{a_{10}} - \frac{9\alpha_1}{8\omega_1}a_{10} - \frac{\alpha_2}{4\omega_1 a_{10}}a_{20}^2 - \frac{1}{2a_{10}}G_1\sin\omega_1\tau),$$

$$\delta_5 = (-\frac{F_1}{2\omega_1 a_{10}}\sin\psi_{10} - \frac{2\alpha_2}{8\omega_1}a_{20}^2(\cos 2\psi_{10}\sin 2\psi_{20} - \sin 2\psi_{10}\cos 2\psi_{20})), \quad \delta_6 = -\frac{2\alpha_2}{4\omega_1}a_{20}a_{21},$$

$$\delta_7 = -\frac{2\alpha_2}{8\omega_1}a_{20}^2(\sin 2\psi_{10}\cos 2\psi_{20} - \cos 2\psi_{10}\sin 2\psi_{20}),$$

$$\delta_8 = (\frac{2\beta_2}{8\omega_2}a_{20}a_{10}^2(\cos 2\psi_{10}\cos 2\psi_{20} + \sin 2\psi_{10}\sin 2\psi_{20}),$$

$$\delta_9 = -(\frac{1}{2}\mu + \frac{1}{2}G_2\cos\omega_2\tau),$$

$$\delta_{10} = (\frac{F_2}{2\omega_2}\cos\psi_{20} - \frac{2\beta_2}{8\omega_2}a_{20}a_{10}^2(\sin 2\psi_{10}\sin 2\psi_{20} + \cos 2\psi_{10}\cos 2\psi_{20})), \quad \delta_{11} = -(\frac{2\beta_2}{4\omega_2}a_{10}),$$

$$\delta_{12} = -(\frac{2\beta_2}{8\omega_2}a_{10}^2(\cos 2\psi_{10}\sin 2\psi_{20} - \sin 2\psi_{10}\cos 2\psi_{20})),$$

$$\delta_{13} = (\frac{\sigma_2}{a_{20}} - \frac{9\beta_1}{8\omega_2}a_{20} - \frac{\beta_2}{4\omega_2 a_{20}}a_{10}^2 - \frac{1}{2a_{20}}G_2\sin\omega_2\tau),$$

$$\delta_{14} = -(\frac{F_2}{2\omega_2 a_{20}}\sin\psi_{20} + \frac{2\beta_2}{8\omega_2}a_{10}^2(\sin 2\psi_{10}\cos 2\psi_{20} - \cos 2\psi_{10}\sin 2\psi_{20}))$$

Coefficients of equation (58)

$$r_1 = (-\delta_9 - \delta_{14} - \delta_1 - \delta_{15}),$$

$$r_2 = (-\delta_{12}\delta_7 - \delta_4\delta_2 - \delta_{11}\delta_3 + \delta_1\delta_{14} + \delta_5\delta_9 + \delta_1\delta_9 - \delta_{10}\delta_{13} - \delta_8\delta_6 + \delta_5\delta_{14} + \delta_9\delta_{14}),$$

$$r_3 = (-\delta_1\delta_9\delta_{14} - \delta_1\delta_5\delta_9 + \delta_1\delta_{12}\delta_7 - \delta_{12}\delta_6\delta_{10} + \delta_{12}\delta_7\delta_9 - \delta_1\delta_5\delta_{14} + \delta_4\delta_2\delta_{14} + \delta_1\delta_8\delta_6 - \delta_8\delta_{13}\delta_7 + \delta_4\delta_2\delta_9 - \delta_4\delta_{12}\delta_3 - \delta_5\delta_9\delta_{14} + \delta_5\delta_{10}\delta_{13} - \delta_{11}\delta_2\delta_7 + \delta_8\delta_6\delta_{14} + \delta_{11}\delta_3\delta_5 - \delta_{11}\delta_3\delta_9 + \delta_1\delta_{10}\delta_{13}),$$

$$r_4 = (\delta_1\delta_5\delta_9\delta_{14} - \delta_4\delta_2\delta_9\delta_{14} - \delta_{11}\delta_3\delta_5\delta_9 - \delta_1\delta_5\delta_{10}\delta_{13} + \delta_4\delta_2\delta_{10}\delta_{13} + \delta_1\delta_{12}\delta_6\delta_{10} + \delta_1\delta_8\delta_{13}\delta_7 - \delta_1\delta_8\delta_6\delta_{14} - \delta_{11}\delta_2\delta_6\delta_{10} + \delta_{11}\delta_2\delta_7\delta_9 + \delta_1\delta_{12}\delta_7\delta_9 + \delta_4\delta_{12}\delta_3\delta_9 + \delta_{11}\delta_8\delta_6\delta_3 - \delta_4\delta_8\delta_{13}\delta_3)$$